Using Sentinels data in CNN to automatically identify solar power plants in Italy: a comparison of different spectral band combinations

Simone Borra[1], Valentina Niutta[1], Ionel Prunila[2], and Massimo Regoli[3]

[1] University of Rome 'Tor Vergata', Economics Faculty,
borra@uniroma2.it
[2] University of Rome 'Sapienza' Information Engineering, Informatics and Statistics Faculty
ionel.prunila@uniroma1.it
[3] University of Rome 'Tor Vergata', Engineering Faculty,
regoli@uniroma2.it

Abstract. Interest in space data applications has been increasing in recent years due to radical digitalization and technological transitions. Satellite data is considered an innovative data source that contributes to the development of models and decision-making policies on relevant topics, including sustainability and energy-related concerns. In our study, we present an implementation of Sentinel-2 data, which is freely available from the European Space Agency's Copernicus project. We integrate this data into a Faster R-CNN algorithm with the goal of automatically detecting solar power plants. We also compare different spectral band combinations to enhance the algorithm's classification ability in terms of average precision. This paper presents an automated approach to detecting solar power plants within Italian territory. It contributes to providing estimates of the growth of renewable and clean energy in the country, while also generating insights to facilitate informed and optimal decision-making.

Keywords: Sentinel Data; Earth Observation; Faster R-CNN; Object detection; Solar plants

1 Introduction

In recent years, climate change, technological transitions, and big data have garnered significant global attention. Many countries are striving for a carbon-neutral future, intending to prioritize the adoption of Solar Energy as a clean alternative to fossil fuels. They are encouraging the establishment of photovoltaic (PV) plants. However, these efforts lack a comprehensive and consistent database of implemented PV plants. Satellite-based Earth Observation (EO) is recognized as an innovative and complementary data source. When combined with current trends in data processing like Artificial Intelligence (AI), Machine

Learning (ML), and Deep Learning (DL) algorithms, it offers an efficient and cost-effective alternative for obtaining automated, frequent, and consistent results. Space Data for Earth Observation involves collecting information about Earth's physical, chemical, and biological systems using remote sensing technologies. When combined with appropriate research and method development, it offers a unique way to gather information [33]. Within the context of Machine Learning, the Convolutional Neural Network (CNN) emerges as a suitable approach for object detection in input images [2][23]. In this work, we employ a specific type of CNN called Faster Region-based Convolutional Neural Network, or Faster R-CNN. This paper presents an innovative approach to automatically identify solar plants in Italy through the utilization of Satellite Data provided freely by the European Space Agency (ESA) via the Copernicus project [36]. These data are collected by the Sentinels 2 satellites. These satellites fly in tandem in the same orbit and carry an optical instrument payload that captures 13 spectral bands: four at 10m, six at 20m, and three at 60m spatial resolution [37]. Our primary research objective is to leverage Deep Learning techniques for the automated detection of Solar Plants in Italy using Sentinel 2 Satellite Data. The study focuses on two main goals. Firstly, we aim to evaluate the algorithm's ability to detect objects such as solar power plants using Sentinel data with relatively low spatial resolution. Secondly, we seek to enhance classification ability by comparing different combinations of Sentinel spectral bands to the traditional use of RGB images (Red, Green, Blue color channels). These two goals can be further classified into three sub-objectives:

1. Object Detection: We assess the algorithm's capability in identifying Solar Power Plants using freely available Sentinel data, focusing on spectral bands with spatial resolutions of 10m and 20m.
2. Image Augmentation Effect: Our aim is to evaluate how much the image augmentation techniques applied to the training sample influences the algorithm's predictive capacity in terms of both average precision and detection performance.
3. Band Combinations: We compare diverse combinations of Spectral Bands to enhance the algorithm's classification capability, particularly in contrast to visible RGB images.

To achieve these objectives, we created a dataset of one thousand satellite images of PV plants from various regions in Italy. This dataset was then utilized to train a Faster R-CNN model, exploring the impact of image augmentation on prediction performance, and investigating various band combinations. The model's effectiveness was confirmed through validation and testing techniques, leading to automated recognition of PV plants throughout Italy. To assess the model's performance, we employed precision-recall curves and average precision. This study offers an approach to manage vast and complex image datasets by automatically identifying large solar plants present on the Italian soil. The proposed work serves as a foundation that can be expanded upon with other deep learning approaches or combined with alternative information sources.

The structure of the paper is as follows: first, we establish a theoretical background on the utilization of space data in relation to solar energy and the implemented ML models. Subsequently, we define the applied methodology; then, we present and discuss the results before concluding with future recommendations.

2 Literature Background

The transition towards renewable energy is capturing substantial attention from governments and policymakers as a response to global climate change issues. Notably, renewable energy generation, with a specific focus on solar PV generation, has become a prominent subject of research [14]. This growing interest has led to increased attention from both businesses and governments. Governments are compelled to monitor and regulate renewable energy, driving a demand for data concerning solar energy production, development, and the distribution of solar panels. Consequently, the exploration of innovative and automated approaches to monitor and facilitate the distribution of solar panels has become a central theme in the research domain. Satellite data emerges as a valuable resource, offering inputs for model development and data-driven strategies in solar energy management. The utilization of Machine Learning models has gained popularity, harnessing the potential of big data to inform decisions and create more efficient models [21]. Over the past two decades, there has been a significant surge in the advancement and application of diverse ML models in energy systems [21]. In recent times, Convolutional Neural Networks have demonstrated remarkable achievements across various applications, including image classification [9][10][16], object detection [7][22][25], and image segmentation [6][26]. CNNs have exhibited outstanding performance in numerous machine learning and pattern recognition tasks within computer vision [13]. While CNNs tend to excel in analyzing datasets with substantial labeled data, they may be prone to overfitting when working with limited labeled data [13]. Nevertheless, deep learning imaging techniques offer a swift and cost-effective means of identifying distributed photovoltaic arrays, both on the ground and on top of buildings. Accurately identifying the shapes and sizes of photovoltaic arrays is imperative for estimating energy production within a given area [13]. Object detection has been one of the main tasks in computer vision research, involving the identification of a specified object's location within an image using a bounding box [24][29]. The process begins with image preparation, involving the labeling of the object of interest. Such algorithms typically encompass two techniques: image classification and detection. Initially, the algorithm endeavors to predict the presence of the object of interest in the image. If the outcome is affirmative, a bounding box is drawn around it. This bounding box process constitutes a regression challenge, as it involves predicting the pixels belonging to the object of interest. Object detection within satellite imagery poses complexity owing to factors like low pixel resolution and the challenge of detecting small objects within large-scale satellite images. This task introduces multiple challenges related to accuracy and efficiency [28]. Thus, a robust algorithm for automatic object detection from

satellite images is essential, and Deep Learning offers a suitable solution for this purpose. After thoroughly examining the relevant body of literature, we have identified key research objectives that are recurrent in prior studies. The studies can be grouped into several categories: the first cluster of studies centers on the detection of PV plants using remote sensing and data processing methods to automate insights extraction from satellite imagery [11][19]. The second group focuses on leveraging satellite imagery for PV plant monitoring to preempt potential faults [5][15][20]. A third set of papers utilizes higher-resolution satellite images to compare the detection abilities of diverse deep learning techniques in terms of performance accuracy [1][3][8]. The final category involves estimating PV power generation through forecasting solar radiation and cloud cover [4][12][17][27]. To the best of our knowledge, these prior studies have predominantly been conducted in countries such as China, South Korea, Australia, and the USA. While a limited number of applications have been carried out in Africa and a few in Italy and other European nations, there appears to be a research gap that our work aims to address. We endeavor to bridge this gap by employing Sentinel 2 data, which exhibits relatively lower resolution, specifically over Italian territory. Our approach entails training a Faster R-CNN model and providing a comprehensive comparison of distinct spectral bands, extending beyond the conventional RGB visible channels.

3 Methodology

The methodological framework of this study is built upon the implementation of a Faster R-CNN algorithm, trained using a dataset of one thousand satellite images sourced from Sentinel 2. Various software tools were utilized, including EO Browser, MakesenseAI, Jupyter Notebooks, and the Python Programming Language. The execution of this work was carried out on a machine with the following technical specifications: two CPUs - an Intel(R) Xeon(R) E5645, each equipped with 6 hard cores and 12 threads; 80GB of RAM; and a P6000 GPU card with embedded CUDA technology. The CUDA configuration comprises a CUDA Driver version of 10.2, runtime version 8.0, and a CUDA capability major/minor version number of 6.1. The total global memory capacity is 24448 Mbytes.

Drawing from the existing literature, which compares the performance of various DL algorithms [28], CNN emerged as one of the most suitable approaches in terms of performance for image processing tasks, like object detection. Hence, we decided to employ it as the most suitable algorithm for our objectives. Specifically, we implemented a Faster R-CNN, utilizing a pre-trained network [35]. The output of the Faster R-CNN comprises one or more bounding boxes on the image, signifying the existence of one or multiple objects. For each bounding box, an estimation of the probability (score) that the object is present within it is provided.

Our approach followed a systematic procedure, starting from data collection up to the training of the Faster R-CNN model, ultimately leading to the final

results. An illustrative representation of this comprehensive process is presented in Fig. 1, which will be further explained in the subsequent paragraphs

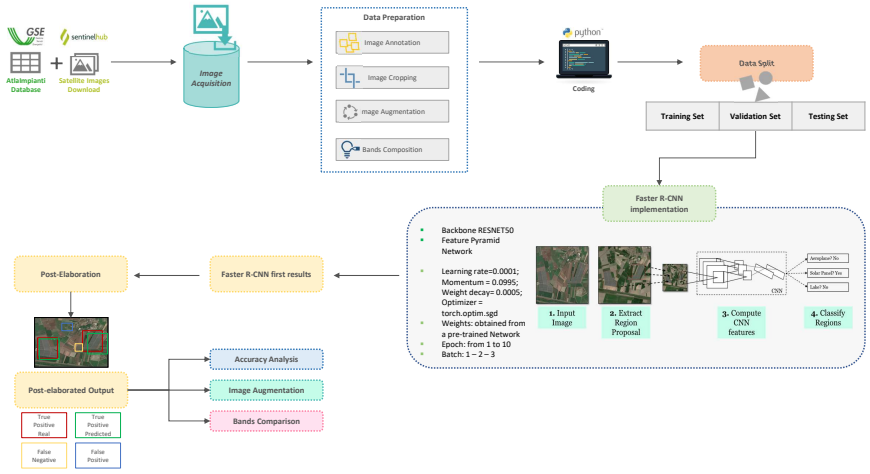

Fig. 1: Methodological flow-chart - Machine Learning workflow

Image Acquisition

First, we utilized a public dataset made available by the company Atlaimpianti (GSE)[32] to identify the locations of the 200 largest solar plants in Italy, updated as of 2020. We established a minimum power capacity threshold of 4950 kilowatts (kw). This dataset aided us to manually identifying the PV plants, which, in turn, allowed us to obtain the corresponding satellite data. It's important to note that although the dataset served its purpose in manual identification, it was not comprehensive and lacked updates, thereby highlighting one of the initial problem statements addressed in this study.

Subsequently, we downloaded the interested images on EO Browser satellites images search engine [31], which is accessible through a user registration. Within EO Browser interface, we selected Sentinel 2 images, which provide high-resolution images in the visible and infrared wavelengths, at Level 2A. Level 2A data ensures high-quality imagery with atmospheric distortions already corrected. During this process, we also configured a maximum Cloud Coverage of 10% to obtain cleaner images. The chosen image selection spanned from January

1, 2022, to May 31, 2022. Additionally, we set the altitude parameter to 500 meters and downloaded the images in high-resolution formats such as KMZ/JPG.

As briefly explained in the introductory paragraph, the sensors carried by satellites can capture images of Earth in different regions of the electromagnetic spectrum, known as bands. Sentinel-2 has 13 bands. A true-color composite utilizes visible light bands, namely red, green, and blue, and assigns them to their corresponding color channels, creating a natural-colored output resembling how the human eye perceives it. Whereas False colour composite comprises at least one non-visible wavelength, such as Infrared. We downloaded images both in True Colours (bands B4, B3, B2) and all individual bands (from B1 to B13). The average dimensions of the downloaded images were 1500x700 pixels.

Image Annotations

After gathering the images, we employed an open-source online software known as MakeSenseAI [38]. Through this tool, we manually applied rectangular labels to each PV plant visible in the downloaded images. These annotations were then stored in Pascal Visual Object Classes (VOC) format, with each annotation saved as an XML file. This process allowed us to generate individual files for each image within the dataset. Each file incorporated the annotated rectangles along with related positional information. These files were easily readable and editable for coding purposes.

Data Preparation and Augmentation

Subsequently, we proceeded with the preparation of the images to serve as input for the Faster R-CNN model. This involved cropping the images to uniform sizes and applying transformations to enhance the diversity of the image dataset. First, we developed a Python code that executed the cropping of each original image. This process resulted in a maximum of 8 squares, each measuring 512x512 pixels. Each square contained at least one PV plant within its boundaries. To enriching the dataset, we created new images by implementing specific transformations to the original images. The transformations included Horizontal Flip, Vertical Flip and Image Rotation in multiples of 90 degrees. We randomly applied a minimum of two out of the three mentioned transformations to each cropped image.

Data Splitting

Once dataset has been prepared, we split it into three distinct sets: Training, Validation and Test. The specifics of this division are summarized in Table 1, which shows the number of images in each sample and the corresponding percentage split. This information is reported for both the dataset consisting solely of the original images, and the dataset that includes images transformed using the Image Augmentation technique. The test sample exclusively consists of original images and does not include any images subjected to augmentation.

	Original Dataset		With Image Augmentation	
Sets	**N. of images**	**% of split**	**N. of images**	**% of split**
Training	413	67%	826	72%
Validation	111	18%	222	19%
Test	96	15%	96	8%
Total	620	100%	1144	100%

Table 1: Description of the sample splitting

Deep learning model for object detection: Architecture and Configuration

Regarding the algorithm's architecture, as previously mentioned, we employed a Faster R-CNN, i.e. Region based Convolutional Neural Network [30]. This architecture functions by extracting a feature map from the convolutional layers and subsequently making predictions about the presence of objects, along with predicting the respective bounding boxes. The loss function used during the training and validation steps, comprehends two weighted main terms: one related to the regression part (for the localization of bounded boxes) and one related to the classification aspect (the classification of bounded boxes). Different appealing properties justify our choice of this architecture:

- Region proposal and object detection CNNs into a single scheme;
- high speed of computation due to weight sharing mechanisms.

In particular, we used as backbone RESNET50 with pre-trained weights provided by [35]. The optimization for the weights has been carried out via stochastic gradient descent and a backpropagation technique. The configuration of the algorithm encompasses parameter setup, weight assignment for training, selection of the number of data epochs, and the batch size for loading data into the network. Below, we outline the specific configuration used:

- Learning rate at 0.0001;
- Momentum at 0.0995;
- Weight decay at 0.0005;
- Optimizer is a `torch.optim.sgd`;
- Weights are obtained from a pre-trained network;
- Tensors which allows to consider only 3 bands as input;
- Batches used are from 1 to 3;
- Epochs applied range from 1 to 10.

Post-Elaboration

Following the prediction phase, we opted to implement a treatment of the predicted bounding boxes. This strategy was made to mitigate their redundancy and

enhance precision and clarity within the obtained results. To achieve this, we assess whether multiple predicted bounding boxes pertain to the same solar plant. Subsequently, we compute the union of these boxes and create a larger encompassing bounding box. The cumulative score of these overall boxes is determined by averaging the scores of individual pixels within the predicted bounding boxes. Each pixel's score is derived from the maximum value among all the prediction bounding boxes that encompass it. This procedure yields two main benefits: it simplifies the output and enhances the overall Average Precision. However, a potential drawback should be acknowledged: it may create a new bounding box containing empty spaces given that the union of boxes might not form a perfectly rectangular shape. Fig. 2 displays the pre and post elaboration procedure.

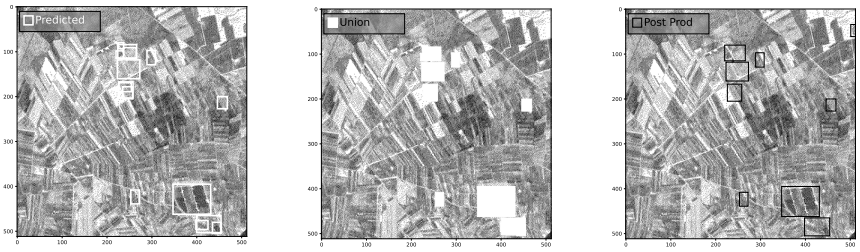

Faster R-CNN output Union of Boxes Post-Elaboration result

Fig. 2: Post-Elaboration procedure

Metrics for Accuracy Analysis

To compare the results, we utilized specific metrics that allowed to distinguish between True Positive (TP), True Negative (TN), False Positive (FP) and False Negative (FN) cases. These metrics also enabled performance evaluation in terms of Precision, Recall, and Average Precision. Initially, we relied on the Intersection over Union (IoU) measurement, which is defined as the ratio between the area of overlap between the True and Predicted labels over the area of their union. It allowed to set thresholds to recognise TP, TN, FP, FN. Furthermore, we computed Precision and Recall scores. Precision signifies the proportion of actual PV plants among all the predicted positives, while Recall indicates the proportion of PV plants correctly classified as positive.

Then, we sorted the scores of predicted boxes in ascending order and computed the two values for each percentile, obtaining the Precision-Recall Curve. The performance measure through which we can compute the comparison between the different combinations of spectral bands is the Average Precision (AP). This index quantifies the area under the P-R Curve (PR AUC). It is computed by

segmenting recall values evenly to 11 parts and then calculate the mean of corresponding precisions. The method used is called 11 points interpolated precision recall curve [34]. We conducted all the experiments and compare the results. To ensure a more robust estimation of AP, we introduced a 7-fold cross-validation approach, thereby scrutinizing the cross-validated results.

4 Results and Discussions

In this section, we present the results obtained using Faster R-CNN on our dataset of PV plant images from various regions in Italy, created from Sentinel-2 images. We will discuss the algorithm's capability to detect PV plants, primarily based on Average Precision, while assessing the impact of image augmentation on performance and the influence of batch size. Additionally, we will compare different combinations of bands in terms of Average Precision. The presentation of results is organized into subsections, aligning with the initially declared research objectives. Initially, we will discuss the results without applying cross-validation, and subsequently, we will explore the analysis of cross-validated results.

Object Detection

The satellite images used as inputs are characterized by a relatively low spatial resolution, ranging from 10m to 20m depending on the specific band.

This implies that the predictive performance of PV plant detection cannot be compared to applications using high-resolution or aerial images. Therefore, resolution becomes a crucial factor affecting the algorithm's predictive capabilities.

For the same reason, we can assert that alternative approaches, such as semantic segmentation [5], can be affetcted, as it would be challenging to clearly distinguish every individual pixel belonging to a solar plant from those that are not.

After the training and test phases of the Faster R-CNN, the highest performance achieved is an average precision of 0.79. This result can be considered a promising starting point for the utilization of Sentinel 2 images in solar power plant detection. It underscores the novelty of this study, which pioneers an analysis based on low-resolution image data. It's important to note that the predicted results are based on rectangular bounding boxes.

Fig. 3 presents an illustrative comparison of predicted labels versus true labels, showcasing the algorithm's capability in detecting solar power plants.

Image Augmentation Effect

In this results section, we explore the impact of image augmentation on Average Precision by comparing the AP obtained from the original dataset with one that includes transformed images. As previously documented in the literature, augmenting the original dataset by adding transformed images typically enhances

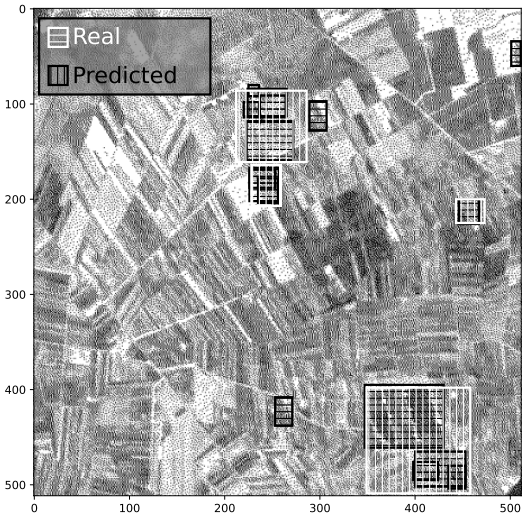

Fig. 3: Objects Detection

the algorithm's object detection capabilities. Thus, it demonstrates a positive effect on performance.

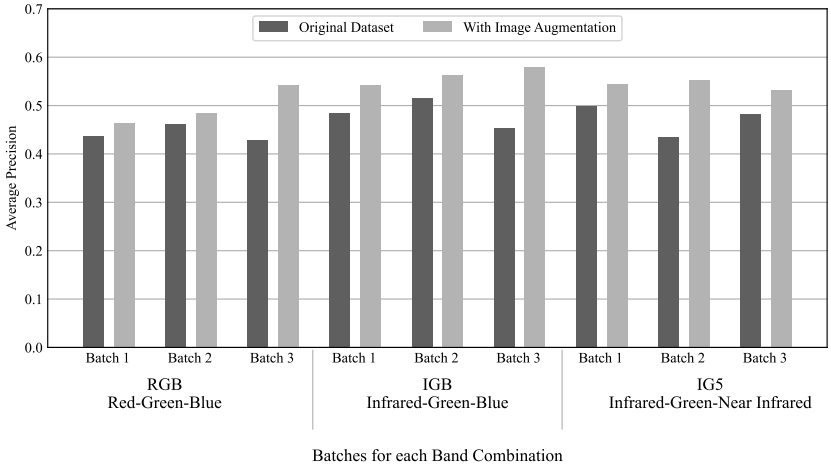

Fig. 4: Image augmentation effect by Band Combinations

Fig. 4 illustrates our analysis of image augmentation, considering three different batch levels and three particularly interesting cases of spectral band combinations: RGB bands (B2, B3, B4 at 10m resolution), Infrared-Green-Blue (B8, B3, B2 at 10m resolution), and Infrared-Green-Near Infrared (B8, B3 at 10m resolution and B5 at 20m resolution). These specific band combinations were selected to provide a comprehensive representation of various image characteristics, including the True Colors visible effect, the impact of infrared, and near-infrared at different spatial resolutions. The key findings from Fig. 4 reveal that average precision consistently increases with image augmentation, underscoring its significant positive effect on performance, regardless of the band combination and batch size. Notably, the highest improvement is observed in the combination that includes the Infrared spectral band at a 10m resolution.

Cleaning up the dataset

After conducting a thorough review of the entire dataset, we identified and rectified missing or incorrect labels, particularly for panels that were inaccurately labeled during the initial phase. Subsequently, we re-executed the cropping procedure to align with the corrected labels. The outcomes of this process are detailed in Table 2. This meticulous adjustment has significantly improved precision, benefiting both the learning and test phases. Consequently, for the remainder of this article, we exclusively present results pertaining to the augmented version of the new dataset.

	Original Dataset		**With Image Augmentation**	
Sets	**N. of images**	**% of split**	**N. of images**	**% of split**
Training	500	72%	1000	77%
Validation	100	14%	200	15%
Test	100	14%	100	8%
Total	700	100%	1300	100%

Table 2: Description of the updated sample splitting

Band Comparison by Average Precision

The primary findings of this study revolve around the comparison of AP over different spectral bands. It is imperative to emphasize that the utilization of Sentinel 2 images provides access to 13 spectral bands, each possessing distinct characteristics compared to the traditional visible bands. Despite the limitation

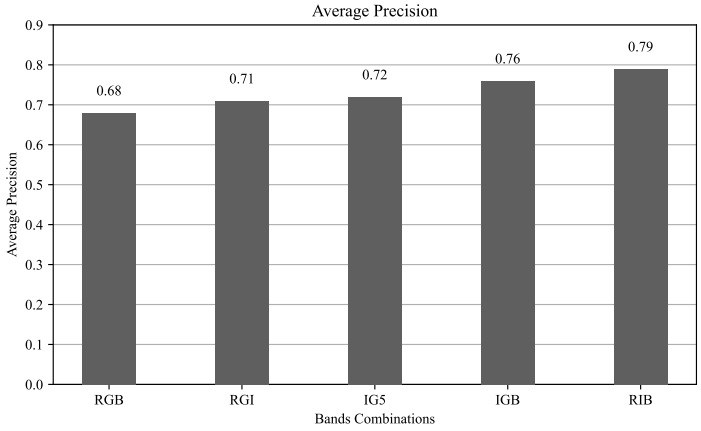

Fig. 5: Average Precision by Band combination

of low spatial resolution, these diverse spectral bands enable us to investigate the presence of PV plants effectively

The central idea behind this study is that PV plants exhibit a spectral signature primarily associated with red and infrared bands. Consequently, employing a different combination of spectral bands, as opposed to the conventional RGB visible channels, proves to be more informative. The impact of utilizing various spectral bands was assessed through average precision measurements conducted at batch level 2. Fig. 5 provides the results obtained by the Faster R-CNN on the test sample. Notably, the best result, with an average precision of 0.79, was achieved using the band combination comprising Red-Infrared-Blue (RIB). This outcome underscores the significance of the Infrared spectral band in effectively detecting PV plants. Additionally, the inclusion of both the red and infrared bands significantly enhances the algorithm's performance.

7-Folds Cross Validation Average Precision

After comparing the results obtained by the Faster R-CNN on the test sample, it became evident that the combination of bands yielding the highest performance in terms of average precision is the one comprised of the RIB bands. Building upon this finding, we opted to employ a 7-fold cross-validation approach to obtain a more robust estimation of AP (as outlined in Table 3). This approach also aimed to validate the superior performance of the RIB bands when contrasted with the RGB and RGI configurations.

The 7-fold cross-validation procedures were executed using all 700 original images, without augmentation (as indicated in Table 2). These images were divided into blocks of 100, with the remaining images, including the augmented ones, being randomly shuffled between training and validation sets. This ensured

that all processes shared the same image configuration, enhancing the reliability of the results. In conclusion, the outcomes of the 7-fold cross-validation estimations, presented in Table 3, confirm the effectiveness of the RIB combination in achieving the best results in the detection of PV plants.

Bands	**7-folds AP**
RIB	0.79
RGB	0.71
RGI	0.65

Table 3: 7-Folds Cross Validation Average Precision

5 Conclusions

Many countries face a significant challenge in maintaining a comprehensive and consistent database of implemented photovoltaic plants. Consequently, there is a pressing need for automated approaches to bridge this information gap. The body of research on solar panel applications has highlighted how the choice of network architecture backbone doesn't appear to significantly impact performance. This underscores the notion that object detection using satellite data is more influenced by the quality and quantity of available data rather than the specific model architecture employed.

Summarizing the key findings of this study, several remarkable insights emerge. Firstly, the effectiveness of image augmentation becomes evident, as the insertion of transformed images into the training set consistently yields improved results in the test set. This improvement in terms of enhanced Average Precision remains consistent across different batch and band combinations. Additionally, the selection of specific band combinations does indeed impact the algorithm's performance, enhancing the characteristics of identified objects. One striking outcome is the superior performance of the RIB combination in detecting PV plants compared to the RGB combination. This conclusion underscores the significant improvements introduced by the use of band Infrared in elevating the average precision for PV plant detection. Moreover, the utilization of Infrared bands justifies the choice of using Sentinel 2 data and post-processing techniques. These enhancements not only reduce label redundancy but also simplify the visual output, resulting in an overall boost in average precision.

This study offers a valuable opportunity to effectively manage and analyze complex and extensive datasets for automatic PV plant detection across the Italian territory. Furthermore, it contributes to estimating the progress of renewable and clean energy development in the country, potentially aiding policy

makers and companies in making informed decisions. Importantly, the approach developed in this research can be adapted for application in other regions nationally and internationally. It serves as a strong foundation that can be extended with additional deep learning methodologies or integrated with diverse sources of information to further enrich its capabilities.

However, it's crucial to acknowledge the limitations of this research. These limitations encompass the selection of the Faster R-CNN network architecture, as opposed to alternative options like Mask R-CNN [18]. Mask R-CNN offers the advantage of assigning polygonal labels instead of rectangular labels, which can lead to improved precision in object detection. Furthermore, the decision to employ object detection techniques, rather than semantic segmentation, can be attributed to the spatial resolution constraints of the data. Indeed, a noteworthy limitation lies in the relatively lower resolution of the satellite images used in this study, especially when compared to some high-resolution studies in the same domain. This resolution limitation can affect the precision and detail of object detection, potentially impacting the overall accuracy of the results. Lastly, an inherent limitation stems from the possibility of human errors associated with manual label assignment. Human involvement in the labeling process introduces the potential for inconsistencies and inaccuracies, which can influence the reliability of the collected data.

One main recommendation is to broaden the scope of band combinations, moving beyond the current reliance on triples. Such an expansion could potentially unlock deeper insights. Furthermore, there's the prospect of estimating the size of solar plants by employing calculations based on the areas associated with identified objects. This approach promises to provide a more comprehensive understanding of the spatial dimensions of these installations, shedding light on their potential energy production capabilities and overall impact.

Another promising avenue for future exploration involves the integration of various data sources. By combining geographic location and real-time weather conditions, an estimate of energy production could be provided.

References

Bibliography

1. Bazi Y., Melgani F.(2018) *Convolutional SVM Networks for Object Detection in UAV Imagery* IEEE Transactions on Geoscience and Remote Sensing,56;3107,3118
2. Bengio, Y., LeCun, Y., and Hinton, G. (2015). *Deep learning.* Nature 521, 436-444. 10.
3. Castello R., Roquette S., Esguerra M., Guerra A., Scartezzini J.-L.(2019) *Deep learning in the built environment: Automatic detection of rooftop solar panels using Convolutional Neural Networks* Journal of Physics: Conference Series,1343;012034
4. Catalina A., Torres-Barran A., Alaiz C.M., Dorronsoro J.R.(2020) *Machine Learning Nowcasting of PV Energy Using Satellite Data* Neural Processing Letters,52;97,115
5. Costa M.V.C.V., Carvalho O.L.F., Orlandi A.G., Hirata I., Albuquerque A.O., Silva F.V., Guimaraes R.F., Gomes R.A.T., Junior O.A.C.(2021) *Remote sensing*

for monitoring photovoltaic solar plants in brazil using deep semantic segmentation Energies,14;2960
6. Farabet C., Couprie C., Najman L., and LeCun Y. (2013). *Learning hierarchical features for scene labeling,* IEEE Trans. Pattern Anal. Mach. Intell., vol. 35, no. 8, pp. 1915-1929
7. Girshick R., Donahue J., Darrell T., and Malik J. (2016). *Region-based convolutional networks for accurate object detection and segmentation* IEEE Trans. Pattern Anal. Mach. Intell., vol. 38, no. 1, pp. 142-158.
8. Golovko V., Kroshchanka A., Mikhno E., Komar M., Sachenko A.(2021) *Deep convolutional neural network for detection of solar panels* Lecture Notes on Data Engineering and Communications Technologies,48;371,389
9. He K., Zhang X., Ren S., and Sun J. (2015). *Spatial pyramid pooling in deep convolutional networks for visual recognition* IEEE Trans. Pattern Anal. Mach. Intell., vol. 37, no. 9, pp. 1904-1916.
10. He K., Zhang X., Ren S., and Sun J. (2016). *Deep residual learning for image recognition,* in Proc. IEEE Conf. Comput. Vis. Pattern Recogn. (CVPR), pp. 770-778, doi: 10.1109/CVPR.2016.90.
11. Ioannou K., Myronidis D.(2021) *Automatic detection of photovoltaic farms using satellite imagery and convolutional neural networks* Sustainability (Switzerland),13;5323
12. Jang H.S., Bae K.Y., Park H.-S., Sung D.K.(2016) *Solar Power Prediction Based on Satellite Images and Support Vector Machine*. IEEE Transactions on Sustainable Energy,7, 1255-1263
13. Jianxin W. (2020) *Essentials of Pattern Recognition: An Accessible Approach.* Cambridge University Press.
14. Kim B., Suh D., Otto M.-O., Huh J.-S.(2021) *A novel hybrid spatio-temporal forecasting of multisite solar photovoltaic generation* Remote Sensing,13;2605
15. Kosmopoulos P.G., Kazadzis S., El-Askary H., Taylor M., Gkikas A., Proestakis E., Kontoes C., El-Khayat M.M.(2018) *Earth-observation-based estimation and forecasting of particulate matter impact on solar energy in Egypt* Remote Sensing,10;1870
16. Krizhevsky, A., Sutskever, I., and Hinton, G.E. (2012). *Imagenet classification with deep convolutional neural networks.* Adv. Neural Inf. Process. Syst. 1097-110
17. Lago J., De Brabandere K., De Ridder F., De Schutter B.(2018) *Short-term forecasting of solar irradiance without local telemetry: A generalized model using satellite data* Solar Energy,173;566,577
18. Liang S., Qi F., Ding Y., Cao R., Yang Q., Yan W.(2020) *Mask R-CNN based segmentation method for satellite imagery of photovoltaics generation systems* Chinese Control Conference, CCC,2020-July;9189474;5343,5348
19. Malof J.M., Collins L.M., Bradbury K.(2017) *A deep convolutional neural network, with pre-training, for solar photovoltaic array detection in aerial imagery* International Geoscience and Remote Sensing Symposium (IGARSS),2017-July;8127092;874,877
20. Mellit A., Kalogirou S.(2021) *Artificial intelligence and internet of things to improve efficacy of diagnosis and remote sensing of solar photovoltaic systems: Challenges, recommendations and future directions* Renewable and Sustainable Energy Reviews,143;110889
21. Mosavi A., Salimi M., Ardabili S.F., Rabczuk T., Shamshirband S., Varkonyi-Koczy A.R.(2019) *State of the art of machine learning models in energy systems, a systematic review* Energies,12;1301

22. Ouyang W. et al. (2017). *DeepID-Net: Object detection with deformable part based convolutional neural networks,* IEEE Trans. Pattern Anal. Mach. Intell., vol. 39, no. 7, pp. 1320-1334.
23. Pritt M. and Chern, G. (2017). *Satellite image classification with deep learning,* in 2017 IEEE Applied Imagery Pattern RecognitionWorkshop (AIPR), pp. 1-7., doi: 10.1109/AIPR.2017.8457969.
24. Radovic, M.; Adarkwa, O.;Wang, Q. (2017). *Object recognition in aerial images using convolutional neural networks.* J. Imaging,3, 21.
25. Ren S., He K., Girshick R., Zhang X., and Sun J. (2017). *Object detection networks on convolutional feature maps,* IEEE Trans. Pattern Anal. Intell., vol. 39, no. 7, pp. 1476-1481
26. Shelhamer E., Long J., and Darrell T. (2017), *Fully convolutional networks for semantic segmentation,* IEEE Trans. Pattern Anal. Mach. Intell., vol. 39, no. 4, pp. 640-651.
27. Srivastava S., Lessmann S.(2018) *A comparative study of LSTM neural networks in forecasting day-ahead global horizontal irradiance with satellite data* Solar Energy,162;232,247
28. Tahir, A.; Munawar, H.S.; Akram, J.; Adil, M.; Ali, S.; Kouzani, A.Z.; Mahmud, M.A.P. (2022). "Automatic Target Detection from Satellite Imagery Using Machine Learning". Sensors, 22, 1147.
29. Zhang, L.; Shi, Z.; Wu, J. (2015). *A Hierarchical Oil Tank Detector With Deep Surrounding Features for High-Resolution Optical Satellite Imagery.* IEEE J. Sel. Top. Appl. Earth Obs. Remote Sens. 8, 4895-4909
30. Ren S., He K., Girshick R., Sun J. (2015). *Faster R-CNN: Towards Real-Time Object Detection with Region Proposal Networks*, in Advances in neural information processing systems 28 (NIPS 2015) edited by: Cortes C., Lawrence N., Lee D., Sugiyama M., Garnett R., pp. 91-99

Web Site

31. https://apps.sentinel-hub.com/eo-browser/?zoom=10&lat=41.9&lng=12.5
32. https://atla.gse.it/atlaimpianti/project/Atlaimpianti_Internet.html
33. https://joint-research-centre.ec.europa.eu/scientific-activities-z/earth-observation-products_en
34. https://link.springer.com/referenceworkentry/10.1007/978-0-387-39940-9_481
35. https://pytorch.org/vision/main key search *fasterrcnn_resnet50_fpn.html*
36. https://www.copernicus.eu/en
37. https://www.esa.int/Applications/Observing_the_Earth/Copernicus/Sentinel-2
38. https://www.makesense.ai/